1-1-2016

Developmental origins for kidney disease due to Shroom3 deficiency

Hadiseh Khalili
McMaster University Medical Centre

Alexandra Sull
Western University

Sanjay Sarin
McMaster University Medical Centre

Felix J. Boivin
McMaster University Medical Centre

Rami Halabi
Western University

See next page for additional authors

Developmental Origins for Kidney Disease Due to *Shroom3* Deficiency

Hadiseh Khalili,* Alexandra Sull,† Sanjay Sarin,* Felix J. Boivin,* Rami Halabi,† Bruno Svajger,* Aihua Li,* Valerie Wenche Cui,* Thomas Drysdale,†‡ and Darren Bridgewater*§

*Department of Pathology and Molecular Medicine, McMaster University, Hamilton, Ontario, Canada; Departments of †Physiology and Pharmacology and ‡Pediatrics, University of Western Ontario, London, Ontario, Canada; and §Hamilton Center for Kidney Research, St. Josephs Healthcare, Hamilton, Ontario, Canada

ABSTRACT

CKD is a significant health concern with an underlying genetic component. Multiple genome–wide association studies (GWASs) strongly associated CKD with the shroom family member 3 (*SHROOM3*) gene, which encodes an actin-associated protein important in epithelial morphogenesis. However, the role of *SHROOM3* in kidney development and function is virtually unknown. Studies in zebrafish and rat showed that alterations in *Shroom3* can result in glomerular dysfunction. Furthermore, human *SHROOM3* variants can induce impaired kidney function in animal models. Here, we examined the temporal and spatial expression of Shroom3 in the mammalian kidney. We detected Shroom3 expression in the condensing mesenchyme, Bowman's capsule, and developing and mature podocytes in mice. *Shroom3* null (*Shroom3*$^{Gt/Gt}$) mice showed marked glomerular abnormalities, including cystic and collapsing/degenerating glomeruli, and marked disruptions in podocyte arrangement and morphology. These podocyte-specific abnormalities are associated with altered Rho–kinase/myosin II signaling and loss of apically distributed actin. Additionally, *Shroom3* heterozygous (*Shroom3*$^{Gt/+}$) mice showed developmental irregularities that manifested as adult-onset glomerulosclerosis and proteinuria. Taken together, our results establish the significance of Shroom3 in mammalian kidney development and progression of kidney disease. Specifically, Shroom3 maintains normal podocyte architecture in mice *via* modulation of the actomyosin network, which is essential for podocyte function. Furthermore, our findings strongly support the GWASs that suggest a role for SHROOM3 in human kidney disease.

J Am Soc Nephrol 27: 2965–2973, 2016. doi: 10.1681/ASN.2015060621

CKD, defined as an irreversible reduction in GFR, affects ≥10% of the population.[1] Although the etiology of this disease can be broad, there is a clear genetic influence.[2] Furthermore, there exists a clear genetic component in childhood- and adult-onset CKD in common conditions, such as diabetes and hypertension.[3] Although large numbers of genetic loci have been associated with CKD, they still only explain a minority of the heritability.[4] Genome–wide association studies (GWASs) linking CKD and GFR to specific single–nucleotide polymorphisms identified additional loci that may impart susceptibility to CKD. One of the loci, uromodulin, has specific mutations that lead to multiple types of kidney disease, showing that the correlations identified by GWASs can identify important loci.[5] Another locus strongly linked to GFR and CKD that influences serum magnesium levels and serum creatinine levels is shroom family member 3 (*SHROOM3*).[5–7]

Shroom3 is an actin-associated protein that regulates epithelial cell shape and tissue morphogenesis. Shroom3 regulates these developmental processes by binding F actin and regulating its subcellular organization.[8,9] Shroom3 interacts and recruits Rho-kinase (Rock), resulting in the phosphorylation and activation of nonmuscle myosin II (MyoII). Activation of this Rock/MyoII signaling pathway causes localized contraction of actomyosin networks at the apical surface of the cell, resulting in changes in cell morphology.[10] During development, Shroom3 is essential for neural tube closure, gut, and lens morphogenesis[9,11,12]

Received June 5, 2015. Accepted January 14, 2016.

H.K., A.S., T.D., and D.B. contributed equally to this work.

Published online ahead of print. Publication date available at www.jasn.org.

Correspondence: Dr. Thomas Drysdale, Departments of Pediatrics and Physiology and Pharmacology, University of Western Ontario and Children's Health Research Institute, 800 Commissioners Road East, London, ON N6A 5W9, Canada, or Prof. Darren Bridgewater, Pathology and Molecular Medicine, McMaster University Medical Centre, 1200 Main Street West, Hamilton, ON L8N 3Z5, Canada. Email: tadrysda@uwo.ca or Bridgew@mcmaster.ca

In the kidney, *SHROOM3* overexpression in renal allografts is correlated with allograft dysfunction in transplant recipients.[12] Specifically, the intronic single–nucleotide polymorphism (rs17319721), linked to CKD in the GWASs, generates a β–catenin enhancer element that elevates *SHROOM3* expression in a TGF-β1–dependent manner. This increased *SHROOM3* expression enhanced TGF-β1–dependent profibrotic genes, leading to transplant interstitial fibrosis and chronic allograft dysfunction.[12] In a separate study using Fawn–Hooded Hypertensive rats, a model of CKD, numerous protein–coding variants were identified within the *Shroom3* gene, one of which disrupted Shroom3 actin binding. Introgression of a wild-type *Shroom3* gene into the Fawn–Hooded Hypertensive rat partially restored glomerular function.[13] Furthermore, these studies showed that morpholino-mediated knockdown of *shroom3* in zebrafish leads to pronephros dysfunction and podocyte foot process effacement,[13] which were restored by injection of mRNA encoding wild-type rat *Shroom3*.[13] Combined, these studies implicate Shroom3 in kidney function and disease progression.

Defining the normal spatial and temporal expression of Shroom3 is an essential first step in understanding the functional role of Shroom3 in CKD. Because the *Shroom3* heterozygous mutant [*Shroom3*$^{Gt(ROSA)53Sor}$/J] mice contain an *LacZ* reporter gene under the control of the endogenous *Shroom3* promoter, we initially analyzed *Shroom3* endogenous gene expression by performing X-Gal staining.[11] In the developing kidney at embryonic (E) 13.5 and E18.5, robust *LacZ* reporter activity was observed in the condensing mesenchyme and during nephrogenesis, specifically in the developing and maturing podocyte cell layer (Figure 1, A–F). Lower levels of *LacZ* reporter activity were also observed in the developing ureter and collecting duct epithelium (Figure 1, D and E). We were particularly interested in the expression of shroom3 in the podocyte cell layer during nephron formation. Therefore, by performing Shroom3 and WT1 coimmunofluorescence (Figure 1, G–I), co–*in situ* hybridization (Supplemental Figure 1, E–H), and immunohistochemistry (Supplemental Figure 1, A–D), we confirmed expression of Shroom3 in podocytes during kidney development. Expression of Shroom3 was also observed postnatally at 3 months in the medullary collecting ducts and glomeruli (Figure 1, J–L). In adult mice, the glomerular expression was limited to the podocyte cell layer (Figure 1L). Thus, the spatial and temporal expression pattern for Shroom3 in the developing and mature kidney suggests a potential role in podocyte development and/or maintenance.

To understand the significance of Shroom3 function in the kidney, we analyzed kidney histology from *Shroom3* null (*Shroom3*$^{Gt/Gt}$) mice during embryonic development. At E13.5, *Shroom3*$^{Gt/Gt}$ exhibited cystic and collapsing glomeruli (Figure 2D). At E14.5 and E18.5, *Shroom3*$^{Gt/Gt}$ mutants exhibited glomerular atrophy with a dilated Bowman's space (Figure 2, E and F). The collapsing glomeruli at E13.5 would suggest that there would be reduced glomerular number, and analysis of glomerular number at E18.5, indeed, showed a *Shroom3* dose–dependent reduction in the number of glomeruli at E18.5 (Figure 2G). These findings indicate that the glomerular abnormalities early in development lead to degenerating glomeruli and reduced glomerular number at later developmental stages. Importantly, the glomerular defects observed in *Shroom3*$^{Gt/Gt}$ mice were also observed in Shroom3 heterozygous (*Shroom3*$^{Gt/+}$) mice (Supplemental Figure 2, A–L). These abnormalities were very rarely observed in *Wild-type* kidneys at any developmental age (Figure 2, A–C, Supplemental Figure 2, A–C). To gain additional insight into the glomerular abnormalities, we performed scanning electron microscopy (SEM) and transmission electron microscopy (TEM) on *Wild-type* and *Shroom3*$^{Gt/Gt}$ mice at similar stages of glomerular development. In contrast to *Wild-type*, *Shroom3*$^{Gt/Gt}$ showed smaller, rounded, abnormally spaced podocyte cell bodies with marked microvillus transformation (Figure 2, H and I versus Figure 2, L and M). In addition, the foot processes in *Shroom3*$^{Gt/Gt}$ podocytes appeared shorter and disorganized, with reduced interdigitation that appeared less adherent to the underlying capillary network (Figure 2, H and I versus Figure 2, L and M). TEM of *Shroom3*$^{Gt/Gt}$ glomeruli showed disrupted glomerular organization with dilated Bowman's space, podocyte hypocellularity, and disorganized podocyte foot processes (Figure 2, J and K versus Figure 2, N and O). Our findings complement a recent study by Yeo *et al.*,[13] which showed that podocyte-specific knockdown of *Shroom3* results in altered podocyte morphology in the zebrafish pronephros. Furthermore, these mutant zebrafish with podocyte specific knockdown of Shroom3 also exhibited disrupted glomerular filtration barrier integrity.[13] Therefore, we next analyzed integral proteins of the slit diaphragm that establish structural and functional properties of the filtration barrier in the mammalian kidney. Expressions of nephrin, podocin, and synaptopodin in *Shroom3*$^{Gt/Gt}$ mice were all disorganized and lacked the distinctive expression pattern that is observed in *Wild-type* podocytes (Figure 2, P–U). In the *Shroom3*$^{Gt/+}$ mice, nephrin expression appeared more diffuse; however, podocin and synaptopodin appeared unchanged (Supplemental Figure 2, J–L). Quantitative RT-PCR showed the levels of nephrin expression were unchanged in both *Shroom3*$^{Gt/Gt}$ and *Shroom3*$^{Gt/+}$ compared with *Wild-type* (Supplemental Figure 2, M and N). Combined, these data show the importance of Shroom3 in the development and/or maintenance of podocyte morphology and foot process architecture.

The organization and regulation of the podocyte actin cytoskeleton are essential for the formation and maintenance of the podocyte cellular architecture and thus, its function. Because Shroom3 regulates cellular morphology in the neural tube by modulating the actin cytoskeleton,[8] we analyzed the actin organization in *Shroom3*$^{Gt/Gt}$ mutant podocytes. In contrast to *Wild-type*, the distinct apical crescent expression pattern of actin was virtually absent in

Shroom3$^{Gt/Gt}$ podocytes (Figure 3, A and B). Additionally, the *Shroom3*$^{Gt/Gt}$ mutant podocytes exhibited actin expression in a more punctate pattern. These changes are highlighted in a schematic diagram (Figure 3C). In neuroepithelial cells, Shroom3 regulates the apical distribution and activation of actomyosin networks by regulating the Rock/MyoII

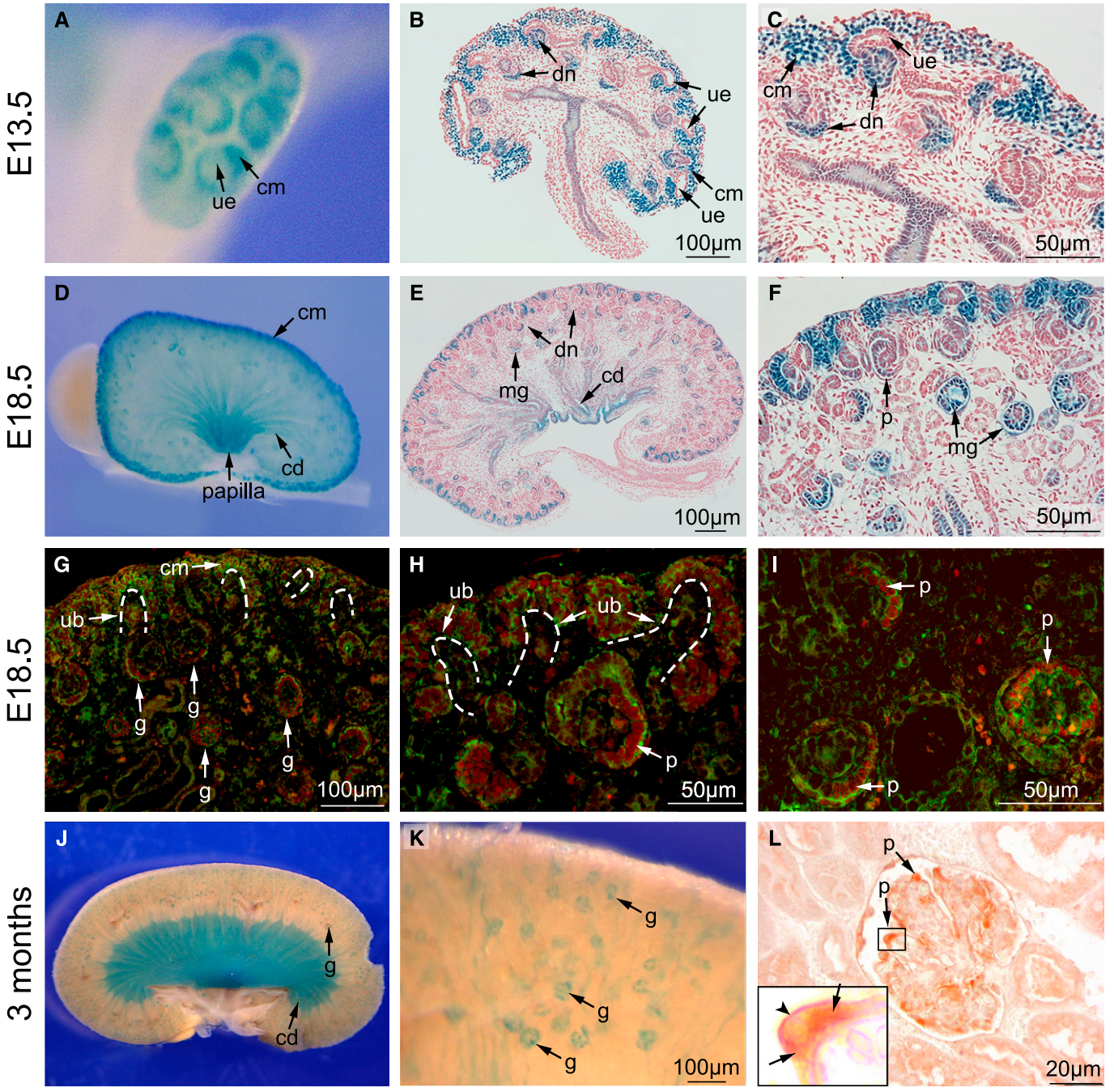

Figure 1. *Shroom3* is expressed in the developing and mature kidney. (A–F) X-Gal staining of E13.5 and E18.5 kidneys representing *Shroom3* endogenous gene expression. At E13.5 and E18.5, *Shroom3* is expressed in medullary collecting duct, condensing mesenchyme adjacent to ureteric epithelium, developing nephrons, and maturing glomeruli in a pattern consistent with the podocyte cell layer. (G–I) Coimmunofluorescence for WT1 and Shroom3 at E18.5 confirms the X-Gal expression in condensing mesenchyme and developing and maturing podocyte cell layers. (J and K) X-Gal staining of a postnatal 3-month-old kidney showing *Shroom3* expression in glomeruli and medullary collecting ducts. (L) At 3 months, *Shroom3* expression is maintained in podocytes in an apical (arrowhead in inset) and cytoplasmic pattern (arrows in inset). cd, Collecting duct; cm, condensing mesenchyme; dn, developing nephron; g, glomerulus; mg, maturing glomerulus; p, podocyte; ub, ureteric bud; ue, ureteric epithelium.

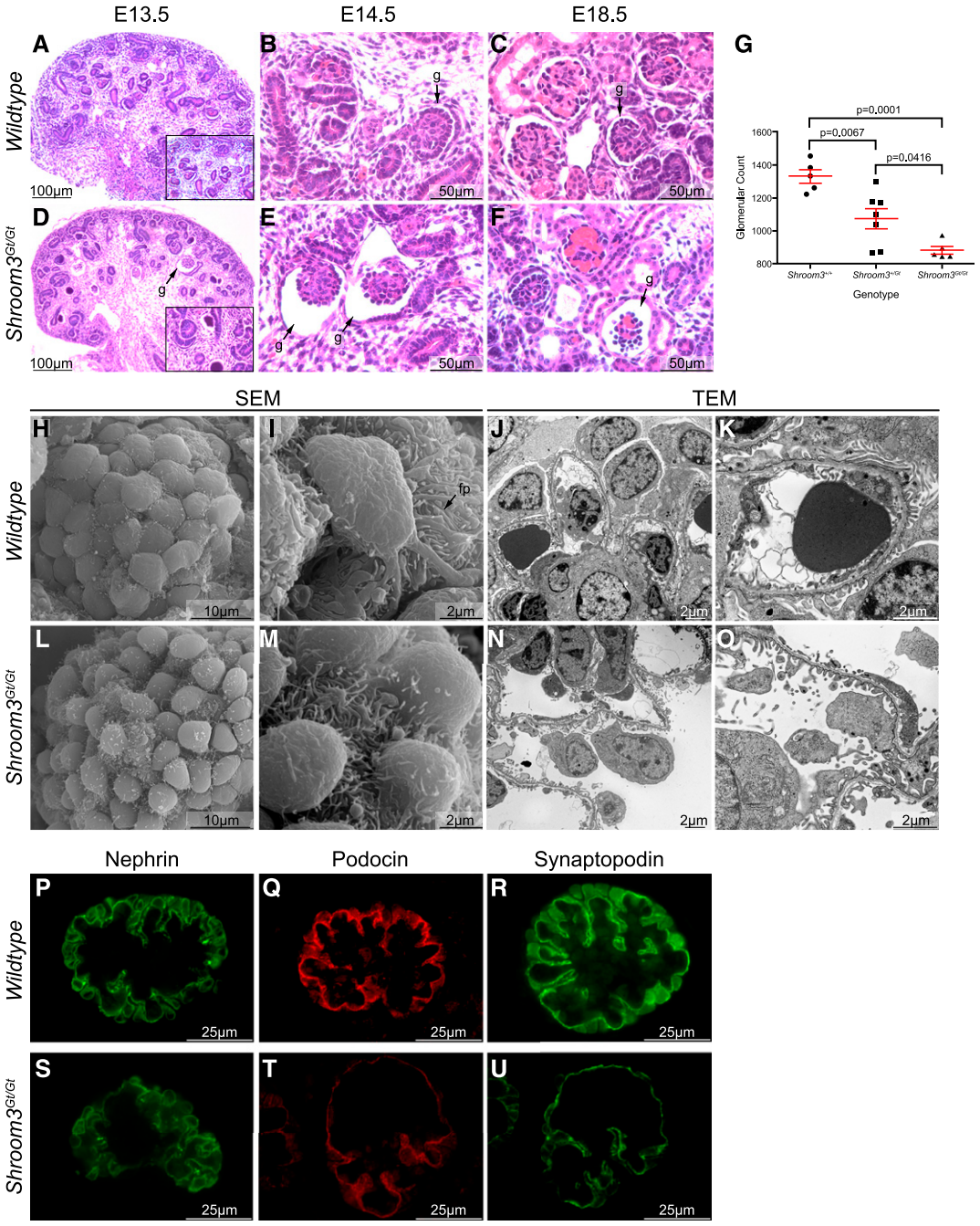

Figure 2. Disrupted glomerulogenesis and podocyte morphology in developing *Shroom3* mutant kidneys. (A–F) Hematoxylin and eosin staining of E13.5, E14.5, and E18.5 *Wild-type* and *Shroom3*$^{Gt/Gt}$ kidney sections. (D, inset) The *Shroom3*$^{Gt/Gt}$ mutants show collapsing and degenerating glomeruli at E13.5 and cystic glomeruli, with a dilated Bowman's capsules at E14.5 and E18.5. (G) Glomerular counting showing a dose-dependent reduction in glomerular number in *Shroom3*$^{Gt/+}$ and *Shroom3*$^{Gt/Gt}$ compared with *Wild-type*. (H–O) Scanning electron microscopy and TEM of comparably aged glomeruli in *Wild-type* and *Shroom3*$^{Gt/Gt}$ mice. (H, I, L, and M) In contrast to *Wild-type*, *Shroom3*$^{Gt/Gt}$ scanning electron microscopy shows small rounded podocyte cell bodies with sporadically arranged podocytes in the glomerular tuft, marked microvillus transformation, and poorly organized foot process interdigitation. Original magnification, ×6000 in H and L; ×20,000 in I and M. (Original magnification, x5000 in J and N; x15,000 in K and O) TEM of *Shroom3*$^{Gt/Gt}$ glomeruli reveals sporadic podocyte arrangement within the glomerulus. Original magnification, ×5000; ×15,000. (P–U) Immunofluorescence of podocyte proteins in embryonic *Wild-type* and *Shroom3*$^{Gt/Gt}$ mutants. (P and S) In contrast to *Wild-type*, nephrin is more diffusely expressed in *Shroom3*$^{Gt/Gt}$ mutant glomeruli. (Q, R, T, and U) Podocin and synaptopodin expression in *Shroom3*$^{Gt/Gt}$ mutant glomeruli shows an irregular thin pattern in the podocyte layer compared with that in *Wild-type*. fp, Foot process; g, glomerulus; SEM, scanning electron microscopy.

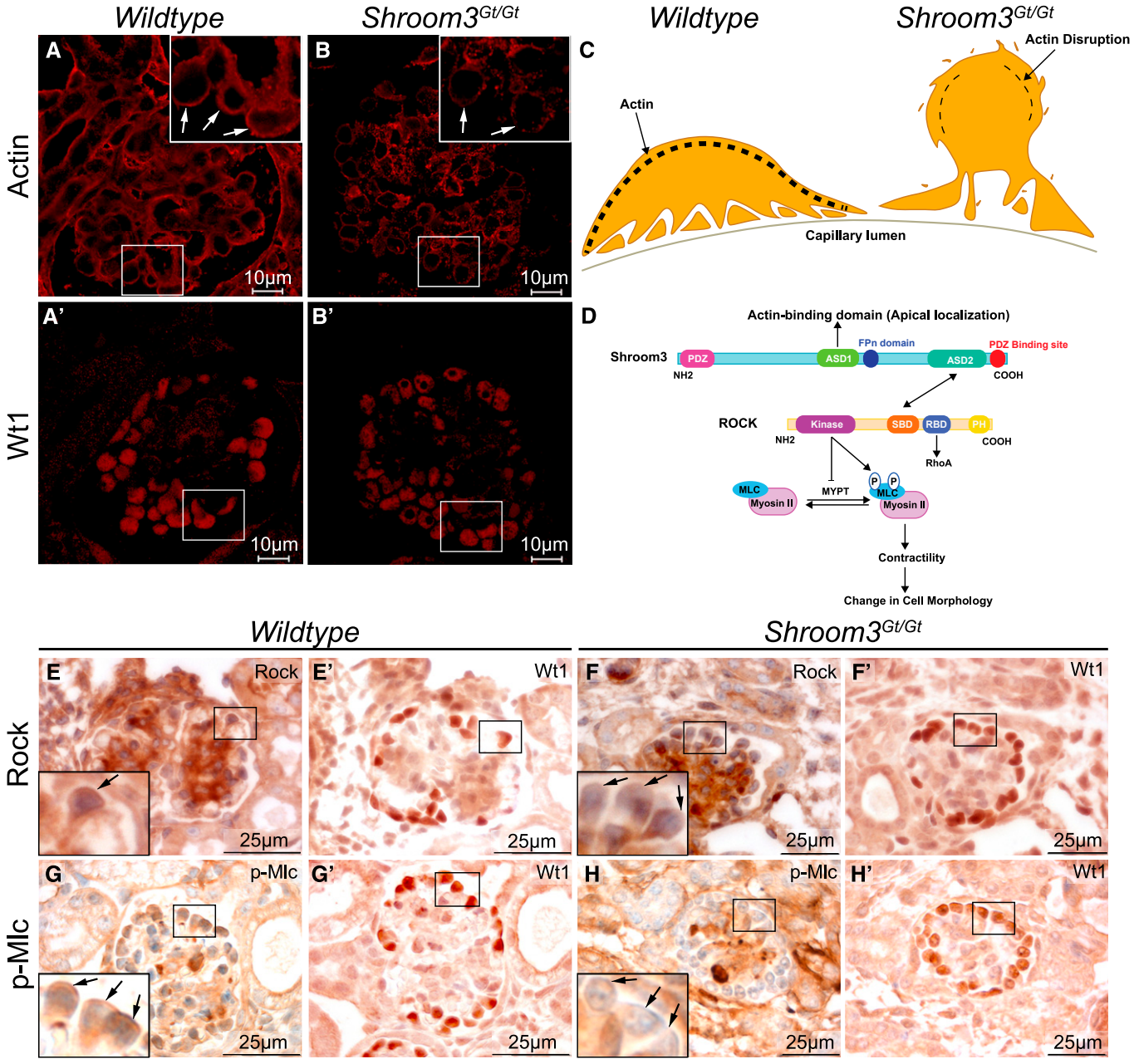

Figure 3. *Shroom3* is required for apical actin distribution *via* Rock/MyoII signaling in podocytes. (A and A′) Immunofluorescence of actin and WT1 on E18.5 serial sections showing an apical crescent pattern of actin expression in *Wild-type* podocytes (arrows in inset). (B and B′) In contrast to *Wild-type*, there is a virtual absence of the apical actin expression in *Shroom3*$^{Gt/Gt}$ podocytes (arrows in inset). (C) A cartoon diagram depicting actin distribution in *Wild-type* and *Shroom3*$^{Gt/Gt}$ podocytes. (D) Schematic model of the actomyosin signaling pathway. (E and E′) E18.5 immunohistochemistry for Rock and WT1 on serial sections showing apical localization of Rock in *Wild-type* podocytes (arrow in inset). (F and F′) In *Shroom3*$^{Gt/Gt}$ mice, there is a loss of apical Rock expression in podocytes (arrows in inset). (G and G′) p-Mlc and WT1 immunohistochemistry on E18.5 serial sections showing apical p-Mlc distribution in *Wild-type* podocytes (arrows in inset). (H and H′) *Shroom3*$^{Gt/Gt}$ mutant podocytes show a loss of apical p-Mlc expression (arrows in inset). MLC, myosin light chain; p-Mlc, phosphomyosin light chain.

signaling pathway, resulting in epithelial cell shape changes (Figure 3D).[14] We assessed Rock1 localization and observed the absence of Rock1 from the apical region in the majority of *Shroom3*$^{Gt/Gt}$ mutant podocytes (Figure 3, E and F). Consistently, the Rock target myosin light chain exhibited a virtual absence of apical phosphorylation in *Shroom3*$^{Gt/Gt}$ mutant podocytes (Figure 3, G and H). Taken together, these data indicate a key regulatory role of Shroom3 in the

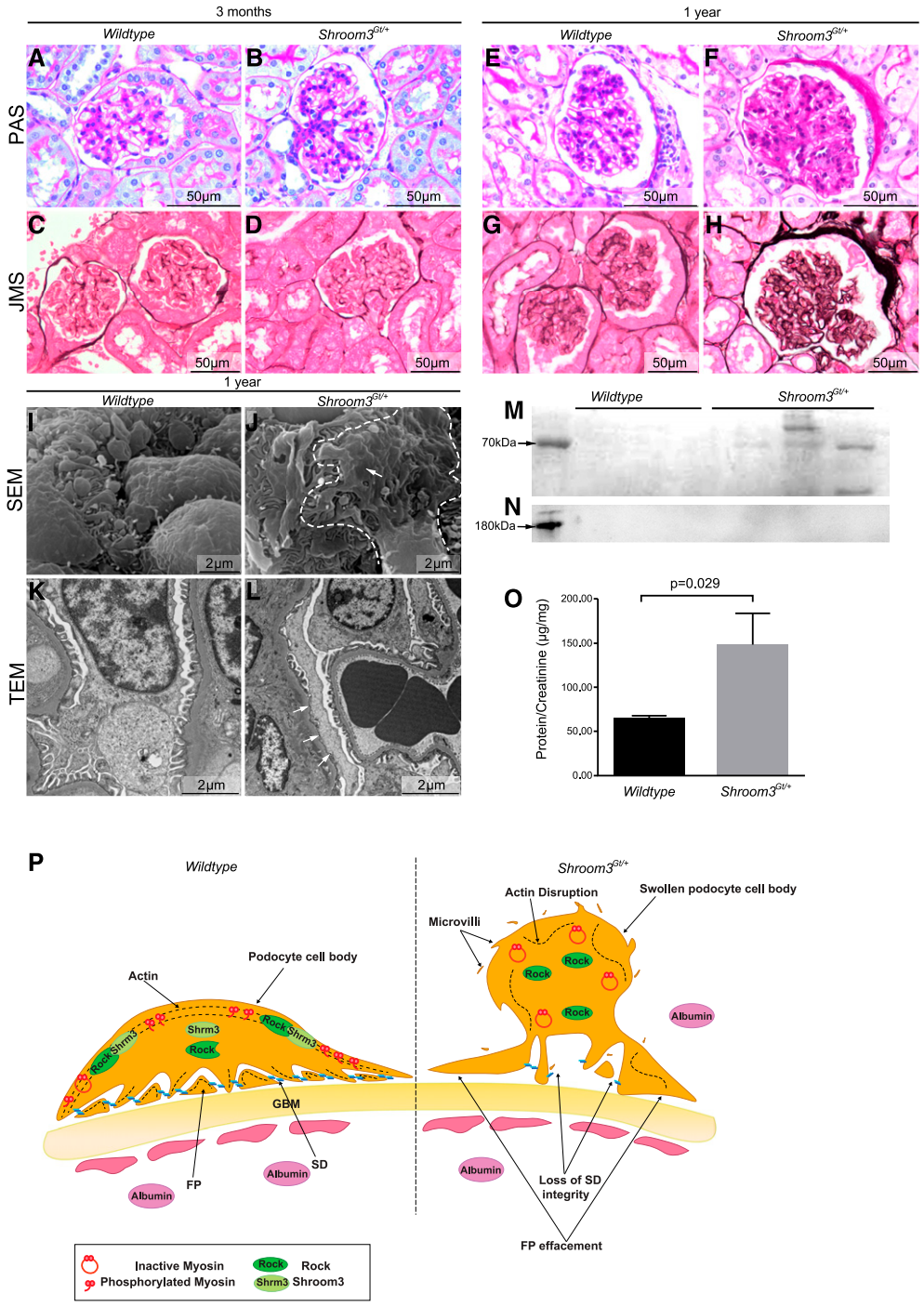

Figure 4. Adult *Shroom3*$^{Gt/+}$ mice exhibit glomerular disease. (A–D) Histopathologic characterization of 3-month-old *Wild-type* and *Shroom3*$^{Gt/+}$ kidneys showed no overt glomerular abnormalities using periodic acid–Schiff (PAS) and Jones Methamine Silver (JMS) staining. (E–H) Histopathologic characterization of 1-year-old kidney tissue shows sclerotic glomeruli and a thickening of the Bowman's capsule in *Shroom3*$^{Gt/+}$ kidneys compared with *Wild-type* kidneys. (I–L) Scanning electron microscopy and TEM of 1-year-old *Wild-type* and *Shroom3*$^{G/+}$ glomeruli show sporadic foot processes flattening and effacement in *Shroom3*$^{G/+}$ mutant kidneys (arrows). (M) Coomassie–stained SDS-PAGE of urine shows albuminuria (a 70-kD albumin band is shown as a positive control) in 1-year-old *Shroom3*$^{Gt/+}$ mice. (N) Western blot analysis for nephrin (a 185-kD nephrin band is shown as a positive control). (O) Analyses of the urinary protein-to-creatinine ratio from 1-year-old *Wild-type* and *Shroom3*$^{Gt/+}$ mice show a significant increase in urinary protein (n=10; P=0.03). (P) Model of the function of *Shroom3* in the podocyte. FP, foot process; GBM, glomerular basement membrane; SD, slit diaphragm; SEM, scanning electron microscopy.

podocyte by modulating actin cytoskeleton organization *via* the Rock/MyoII signaling pathway to establish normal podocyte cytoarchitecture.

Because GWASs implicate Shroom3 in kidney disease, we sought to determine if the developmental abnormalities in *Shroom3*$^{Gt/Gt}$ mice manifest in adult–onset kidney disease. Because of the neonatal lethality of *Shroom3*$^{Gt/Gt}$ mice resulting from exencephaly,[11] adult kidneys from *Shroom3*$^{Gt/+}$ and *Wild-type* littermates were analyzed. Despite the glomerular pathologies in embryonic *Shroom3*$^{Gt/+}$ mice (Supplemental Figure 2, G–I), we did not detect any overt glomerular pathologies or evidence of urinary protein in 3-month-old mice (Figure 4, A–D) (data not shown). Considering that kidney disease is often progressive, we analyzed kidney tissue from 1-year-old *Shroom3*$^{Gt/+}$ kidneys. *Shroom3*$^{Gt/+}$ mutants developed mild glomerulosclerosis characterized by increased matrix deposition and a thickening of the Bowman's capsule (Figure 4, E–H). At the ultrastructural level, scanning electron microscopy revealed sporadic foot process flattening, fusion, and effacement in 1-year-old *Shroom3*$^{Gt/+}$ mice that was confirmed using TEM (Figure 4, I–L). Furthermore, podocyte counting showed a reduced podocyte number per glomerulus in the *Shroom3*$^{Gt/+}$ mice (Supplemental Figure 2, O–Q). Because proteinuria is often associated with podocyte injury, podocyte loss, and glomerulosclerosis,[15] we analyzed urine from 1-year-old *Shroom3*$^{Gt/+}$ mice. We detected varying amounts of albuminuria by SDS-PAGE (Figure 4M) but did not detect any podocyte proteins (Figure 4N). The protein-to-creatinine ratio in *Shroom3*$^{Gt/+}$ mice was increased compared with that in *Wild-type* (Figure 4O).

Taken together, our findings suggest that Shroom3 is required for the development and maintenance of podocyte cytoarchitecture. In the absence of Shroom3, during development, the podocyte morphology is altered, leading to podocyte loss and glomerular degeneration. The interaction of Shroom3 with Rock localizes the complex to the apical region of the podocytes. Here, Rock triggers actomyosin contractility by the phosphorylation and activation of its known downstream target, MyoII. Increased phosphorylation of MyoII induces the formation of a network of apical actin stress fibers and stabilization of the actin cytoskeleton in the apical region of podocytes (Figure 4P). Conversely, the loss of Shroom3 in mutant podocytes results in the failure of Rock localization to the podocyte apical region. Consequently, phosphorylated MyoII is reduced along the apical membrane of podocytes, leading to decreased apical formation of contractile actin-myosin stress fibers. These changes can result in altered podocyte cell body and foot process morphology during development or postnatally culminate in glomerular abnormalities (*i.e.*, sclerosis), dysfunction, and albuminuria.

In a search for new genes that may be associated with kidney disease, GWASs have implicated *SHROOM3* as a potential candidate. Here, we provide experimental evidence to support that role. *Shroom3* is expressed in the podocyte, and it is necessary for developing and/or maintaining the complex podocyte cytoarchitecture. Because a complete loss of *Shroom3* activity would be predicted to be lethal because of its role in neural tube closure, it is important to note that *Shroom3*$^{Gt/+}$ adult mice have indicators of kidney disease. This suggests that potential hypomorphic human *SHROOM3* alleles could directly result in kidney disease or increased susceptibility to CKD from nongenetic causes, such as diabetes.

CONCISE METHODS

Mice

Shroom3$^{Gt(ROSA)53Sor}$/J mice[11] were received from Thomas Drysdale (University of Western Ontario). Animal studies were performed in accordance with Canadian Council for Animal Care and McMaster University institutional guidelines (Animal Utilization Protocol 10–08–55). Genotyping was performed on tail DNA using the following primers: forward primer 5′-GGTGACTGAGGAGTAGAGTCC-3′ and reverse primers 5′-GCAACCACATGGTGGGAGACAAGC-3′ and 5′-GAGTTTGTGCTCAACCGCGAGC-3′.

β-Galactosidase Staining

Whole–mount X-Gal staining was performed on *Wild-type*, *Shroom3*$^{Gt/Gt}$, and *Shroom3*$^{Gt/+}$ embryonic and adult kidneys as described[16] and visualized on a Leica EZ4D Microscope (Leica Microsystems, Buffalo Grove, IL).

In Situ Hybridization

Two–plex *in situ* hybridization was performed using the Affymetrix QuantiGene ViewRNA (Affymetrix, Santa Clara, CA) according to the manufacturer's protocol.

Histology

Whole-kidney tissue was fixed in 4% paraformaldehyde for 24 hours at 4°C, embedded in paraffin, sectioned at 4–6 μm, and stained with hematoxylin and eosin (Sigma-Aldrich, St. Louis, MO), periodic acid–Schiff, and Jones Methamine Silver using standard protocols.

Immunologic Techniques

Immunofluorescence was performed as described.[17] We used the primary antibodies Shroom3 (1:200; Santa Cruz Biotechnology, Santa Cruz, CA), WT1 (1:200; Santa Cruz Biotechnology), nephrin (1:200; R&D Systems, Minneapolis, MN), synaptopodin (1:200; Santa Cruz Biotechnology), podocin (1:200; Sigma-Aldrich), and actin (1:200; Abcam, Inc., Cambridge, MA) overnight at 4°C and secondary antibodies Alexa Fluor 488 or 568 (1:1000 dilution; Invitrogen, Carlsbad, CA). Immunohistochemistry was performed using the Vectastain Elite Avidin-Biotin-Peroxidase Complex Kit as per the manufacturer's instructions (Vector Laboratories, Burlingame, CA) using the anti–goat Shroom3 antibody (1:200; Santa Cruz Biotechnology), phosphomyosin light chain (1:300; Abcam, Inc.), and ROCK1 (1:200; Abcam, Inc.). Immunoreactivity was visualized using 3′-diaminobenzidine (Vector Laboratories). All images were captured by either an Olympus BX60 (Olympus, Tokyo, Japan) or a Nikon 90i-Eclipse Fluorescence Microscope (Nikon, Tokyo, Japan). Confocal images were captured by Zeiss LSM510 Confocal Microscopy (Carl Zeiss GmbH, Jena, Germany).

TEM and Scanning Electron Microscopy

For TEM, whole-embryonic kidneys from *Wild-type* and *Shroom3*$^{Gt/Gt}$ at E18.5 were fixed with 2.5% glutaraldehyde in 0.1 M sodium-cacodylate buffer. Adult kidney cortexes from *Wild-type* and *Shroom3*$^{Gt/+}$ mice at 1 year old were minced to 2-mm cubes and fixed as above. Kidney tissue was postfixed with 1% osmium teroxide, dehydrated using graded ethanol washes, and embedded in epoxy resin. Ultrathin sections were cut and stained with uranyl acetate. Images were viewed using JEOL JEM 1200 EM TEMSCAN (Tokyo, Japan). Images were captured with an AMT 4 Megapixel Digital Camera. For scanning electron microscopy, embryonic and adult kidney tissues were fixed as above and processed for scanning electron microscopy. All electron microscopy imaging and tissue processing were performed at the Electron Microscopy Facility at McMaster University.

Analyses of Mouse Urine

Spot urine samples were collected from *Shroom3*$^{Gt/+}$ (n=5) and *Wild-type* littermates (n=5). Urinary proteins were concentrated using an Amicon Ultra 0.5-ml Centrifugal Filter (NMWL 10 kD; EMD Millipore, Billerica, MA). Proteinuria was qualitatively analyzed by running equal volumes of urine samples on 10% SDS gels followed by Coomassie Brilliant Blue staining. Protein concentration in urine was measured by the Bradford method (microtiter scale; Bio-Rad, Hercules, CA).[18] Urine creatinine was measured in duplicate for each sample (MAK080; Sigma-Aldrich). Urinary protein was normalized to urine creatinine defined as the protein-to-creatinine ratio. For the presence of podocytes in the urine, protein was isolated from urine, and Western blot analysis was performed for nephrin.

Glomeruli and Podocyte Counting

Glomeruli counting was performed as described.[19] Briefly, entire E18.5 kidneys was sectioned at 5 μm and imaged at $\times$10 magnification. Glomeruli were counted in every 10th section from *Wild-type* (n=5), *Shroom3*$^{Gt/+}$ (n=6), and *Shroom3*$^{Gt/Gt}$ (n=5) kidneys. Podocyte counting was performed as described.[20] Briefly, the number of WT1-positive podocytes was counted from 10 glomerular sections from three different *Shroom3*$^{Gt/Gt}$ and *Wild-type* littermates. The number of podocytes was expressed as the mean with standard error of the mean.

Statistical Analyses

Data were analyzed using one-way ANOVA with a *post hoc* Kruskal–Wallis test.

ACKNOWLEDGMENTS

We thank renal pathologist Dr. Iakovina Alexopoulou for her analysis of the renal histology.

This study was supported by startup funds from McMaster University (to D.B.) and grants from the Kidney Foundation of Canada and the National Science and Engineering Research Council.

DISCLOSURES

None.

REFERENCES

1. Price PM, Hirschhorn K, Safirstein RL: Chronic kidney disease and GWAS: "The proper study of mankind is man." *Cell Metab* 11: 451–452, 2010
2. Modem V, Thompson M, Gollhofer D, Dhar AV, Quigley R: Timing of continuous renal replacement therapy and mortality in critically ill children*. *Crit Care Med* 42: 943–953, 2014
3. Parsa A, Kao WH, Xie D, Astor BC, Li M, Hsu CY, Feldman HI, Parekh RS, Kusek JW, Greene TH, Fink JC, Anderson AH, Choi MJ, Wright JT Jr., Lash JP, Freedman BI, Ojo A, Winkler CA, Raj DS, Kopp JB, He J, Jensvold NG, Tao K, Lipkowitz MS, Appel LJ; AASK Study Investigators; CRIC Study Investigators: APOL1 risk variants, race, and progression of chronic kidney disease. *N Engl J Med* 369: 2183–2196, 2013
4. Devuyst O, Knoers NV, Remuzzi G, Schaefer F; Board of the Working Group for Inherited Kidney Diseases of the European Renal Association and European Dialysis and Transplant Association: Rare inherited kidney diseases: Challenges, opportunities, and perspectives. *Lancet* 383: 1844–1859, 2014
5. Köttgen A, Glazer NL, Dehghan A, Hwang SJ, Katz R, Li M, Yang Q, Gudnason V, Launer LJ, Harris TB, Smith AV, Arking DE, Astor BC, Boerwinkle E, Ehret GB, Ruczinski I, Scharpf RB, Chen YD, de Boer IH, Haritunians T, Lumley T, Sarnak M, Siscovick D, Benjamin EJ, Levy D, Upadhyay A, Aulchenko YS, Hofman A, Rivadeneira F, Uitterlinden AG, van Duijn CM, Chasman DI, Paré G, Ridker PM, Kao WH, Witteman JC, Coresh J, Shlipak MG, Fox CS: Multiple loci associated with indices of renal function and chronic kidney disease. *Nat Genet* 41: 712–717, 2009
6. Böger CA, Gorski M, Li M, Hoffmann MM, Huang C, Yang Q, Teumer A, Krane V, O'Seaghdha CM, Kutalik Z, Wichmann HE, Haak T, Boes E, Coassin S, Coresh J, Kollerits B, Haun M, Paulweber B, Köttgen A, Li G, Shlipak MG, Powe N, Hwang SJ, Dehghan A, Rivadeneira F, Uitterlinden A, Hofman A, Beckmann JS, Krämer BK, Witteman J, Bochud M, Siscovick D, Rettig R, Kronenberg F, Wanner C, Thadhani RI, Heid IM, Fox CS, Kao WH; CKDGen Consortium: Association of eGFR-related loci identified by GWAS with incident CKD and ESRD. *PLoS Genet* 7: e1002292, 2011
7. Meyer TE, Verwoert GC, Hwang SJ, Glazer NL, Smith AV, van Rooij FJ, Ehret GB, Boerwinkle E, Felix JF, Leak TS, Harris TB, Yang Q, Dehghan A, Aspelund T, Katz R, Homuth G, Kocher T, Rettig R, Ried JS, Gieger C, Prucha H, Pfeufer A, Meitinger T, Coresh J, Hofman A, Sarnak MJ, Chen YD, Uitterlinden AG, Chakravarti A, Psaty BM, van Duijn CM, Kao WH, Witteman JC, Gudnason V, Siscovick DS, Fox CS, Köttgen A; Genetic Factors for Osteoporosis Consortium; Meta Analysis of Glucose and Insulin Related Traits Consortium: Genome-wide association studies of serum magnesium, potassium, and sodium concentrations identify six loci influencing serum magnesium levels. *PLoS Genet* 6: e1001045, 2010
8. Haigo SL, Hildebrand JD, Harland RM, Wallingford JB: Shroom induces apical constriction and is required for hingepoint formation during neural tube closure. *Curr Biol* 13: 2125–2137, 2003
9. Lee C, Scherr HM, Wallingford JB: Shroom family proteins regulate gamma-tubulin distribution and microtubule architecture during epithelial cell shape change. *Development* 134: 1431–1441, 2007
10. Plageman TF Jr., Chauhan BK, Yang C, Jaudon F, Shang X, Zheng Y, Lou M, Debant A, Hildebrand JD, Lang RA: A Trio-RhoA-Shroom3 pathway is required for apical constriction and epithelial invagination. *Development* 138: 5177–5188, 2011
11. Hildebrand JD, Soriano P: Shroom, a PDZ domain-containing actin-binding protein, is required for neural tube morphogenesis in mice. *Cell* 99: 485–497, 1999
12. Menon MC, Chuang PY, Li Z, Wei C, Zhang W, Luan Y, Yi Z, Xiong H, Woytovich C, Greene I, Overbey J, Rosales I, Bagiella E, Chen R, Ma M, Li L, Ding W, Djamali A, Saminego M, O'Connell PJ, Gallon L, Colvin

R, Schroppel B, He JC, Murphy B: Intronic locus determines SHROOM3 expression and potentiates renal allograft fibrosis. *J Clin Invest* 125: 208–221, 2015
13. Yeo NC, O'Meara CC, Bonomo JA, Veth KN, Tomar R, Flister MJ, Drummond IA, Bowden DW, Freedman BI, Lazar J, Link BA, Jacob HJ: Shroom3 contributes to the maintenance of the glomerular filtration barrier integrity. *Genome Res* 25: 57–65, 2015
14. Nishimura T, Takeichi M: Shroom3-mediated recruitment of Rho kinases to the apical cell junctions regulates epithelial and neuroepithelial planar remodeling. *Development* 135: 1493–1502, 2008
15. Shi S, Yu L, Chiu C, Sun Y, Chen J, Khitrov G, Merkenschlager M, Holzman LB, Zhang W, Mundel P, Bottinger EP: Podocyte-selective deletion of dicer induces proteinuria and glomerulosclerosis. *J Am Soc Nephrol* 19: 2159–2169, 2008
16. Sarin S, Boivin F, Li A, Lim J, Svajger B, Rosenblum ND, Bridgewater D: β-Catenin overexpression in the metanephric mesenchyme leads to renal dysplasia genesis via cell-autonomous and non-cell-autonomous mechanisms. *Am J Pathol* 184: 1395–1410, 2014
17. Bridgewater D, Di Giovanni V, Cain JE, Cox B, Jakobson M, Sainio K, Rosenblum ND: β-catenin causes renal dysplasia via upregulation of Tgfβ2 and Dkk1. *J Am Soc Nephrol* 22: 718–731, 2011
18. Pérez de Lema G, Maier H, Nieto E, Vielhauer V, Luckow B, Mampaso F, Schlöndorff D: Chemokine expression precedes inflammatory cell infiltration and chemokine receptor and cytokine expression during the initiation of murine lupus nephritis. *J Am Soc Nephrol* 12: 1369–1382, 2001
19. Das A, Tanigawa S, Karner CM, Xin M, Lum L, Chen C, Olson EN, Perantoni AO, Carroll TJ: Stromal-epithelial crosstalk regulates kidney progenitor cell differentiation. *Nat Cell Biol* 15: 1035–1044, 2013
20. Wanner N, Hartleben B, Herbach N, Goedel M, Stickel N, Zeiser R, Walz G, Moeller MJ, Grahammer F, Huber TB: Unraveling the role of podocyte turnover in glomerular aging and injury. *J Am Soc Nephrol* 25: 707–716, 2014

This article contains supplemental material online at http://jasn.asnjournals.org/lookup/suppl/doi:10.1681/ASN.2015060621/-/DCSupplemental.